

# Highly-Sensitive Polymer Optical Fiber SPR Sensor for Fast Immunoassay

Ying WANG<sup>1,2</sup>, Xing RAO<sup>1,2</sup>, Xun WU<sup>1,2</sup>, George Y. CHEN<sup>1,2\*</sup>, Changrui LIAO<sup>1,2</sup>, Mateusz Jakub SMIETANA<sup>3</sup>, and Yiping WANG<sup>1,2\*</sup>

<sup>1</sup>Key Laboratory of Optoelectronic Devices and Systems of Ministry of Education/Guangdong Province, College of Physics and Optoelectronic Engineering, Shenzhen University, Shenzhen 518060, China

<sup>2</sup>Shenzhen Key Laboratory of Photonic Devices and Sensing Systems for Internet of Things, Guangdong and Hong Kong Joint Research Centre for Optical Fibre Sensors, Shenzhen University, Shenzhen 518060, China

<sup>3</sup>Division of Microsystem & Electronic Materials Technology, Institute of Microelectronics & Optoelectronics, Warsaw University of Technology, Koszykowa 75, 00-662 Warsaw, Poland

\*Corresponding authors: George Y. CHEN and Yiping WANG  
E-mails: gychen@szu.edu.cn and ypwang@szu.edu.cn

**Abstract:** A new type of human immunoglobulin G (IgG) sensors based on the surface plasmon resonance (SPR) in the low refractive index (RI) plastic optical fiber (POF) and an antibody immobilization method is presented. A 50-nm-thick gold film was formed on the polished D-shaped fiber surface by magnetron sputtering. The RI response of the POF sensor is 30 049.61 nm/RIU, which is 26.5 times higher than that of single mode fiber (SMF) SPR sensors. The proposed SPR biosensor can be developed by simple and rapid modification of the gold film with 11-mercaptopropionic acid (MPA). Upon immobilization of the goat anti-human IgG antibody, the resonance wavelength shifts by 11.2 nm. The sensor can be used to specifically detect and quantify the human IgG at concentrations down to 245.4 ng/mL with the sensitivity of 1.327 7 nm per  $\mu\text{g/mL}$ , which offers an enhancement of 12.5-fold compared to that of the conventional SMF based SPR sensors. The proposed device may find the potential applications in the case of use at the point of care.

**Keywords:** Optical fiber biosensor; surface plasmon resonance; antibody immobilization; side-polished fiber; plastic optical fiber

---

Citation: Ying WANG, Xing RAO, Xun WU, George Y. CHEN, Changrui LIAO, Mateusz Jakub SMIETANA, *et al.*, "Highly-Sensitive Polymer Optical Fiber SPR Sensor for Fast Immunoassay," *Photonic Sensors*, 2024, 14(4): 240413.

---

## 1. Introduction

Immunoglobulin G (IgG) is an important antibody that protects the body from viruses. It is clinically important for understanding the humoral immune function and diagnosing various diseases such as immune enhancement [1], immunodeficiency [2], infection [3], and autoimmunity [4]. The IgG

concentration clinically reflects the immune status of the body against specific pathogens, and thus a rapid and accurate method is needed to quantify the IgG concentration. Compared to the traditional methods such as Enzyme-linked immunosorbent assay (ELISA) [5] and radioimmunoassay [6], optical sensors offer natural advantages, such as the small size, fast response, label-free, and

---

Received: 9 November 2023 / Revised: 31 January 2024

© The Author(s) 2024. This article is published with open access at Springerlink.com

DOI: 10.1007/s13320-024-0729-x

Article type: Regular

contamination-free [7–9]. There are various types of optical based biosensors [10], including interferometers [11], gratings [12], and surface plasmon resonance (SPR) devices [13]. Among these, the SPR is currently proving to be one of the most viable technologies for developing label-free, point-of-care, and high-throughput biosensors [14, 15].

Conventional SPR sensors have a built-in Kretschmann configuration that relies on large optical elements, resulting in high operating costs and challenges with miniaturization [16]. In this regard, emerging specialty fibers exhibit many outstanding features (e.g., high sensitivity, low cost, lightweight, distributed sensing potential, and small size) that can be used to develop SPR sensors [17–20]. To date, the meaningful work has been carried out to improve existing fiber optic SPR sensor configurations by employing specialty fibers. Depending on the profile of the detection area, fiber-optic SPR sensors use different types of optical fibers or configurations as the sensor head, such as the D-shaped probe [21], U-shaped probe [22], tapered fibers [23], and microfibers [24, 25]. Among these, the D-shaped sensing structure leads to a range of benefits (e.g., high sensitivity, easy surface functionalization, and large detection area). To date, the great efforts have been made to promote the development of fiber-optic SPR sensors. For example, in 2019, J. X. Sun *et al.* [26] proposed a gold/graphene composite membrane D-POF sensor with a sensitivity of 1 539 nm/RIU in the ethanol solution. In 2020, N. Cennamo *et al.* [27] proposed an SPR sensor based on a D-shaped micro/nano fiber probe. In 2021, F. Wang *et al.* [28] proposed a fiber-optic SPR label-free biosensor based on a gold nanoparticle-old film “hot spot” model in the near-infrared. However, a leap forward in clinical applications has elevated the requirements for the sensitivity and stability of fiber-optic SPR sensors.

In recent years, various means to improve SPR based sensors have been reported. Just to name a

few, X. Xiong *et al.* [29] proposed the modification of the graphene oxide on the surface to improve the sensitivity in biological solutions up to 2 715.1 nm/RIU. A. K. Sharma *et al.* [30] proposed a metal and a 2-dimensional material structure to improve the sensitivity. C. Li *et al.* [31] proposed the Au/Al<sub>2</sub>O<sub>3</sub> based multilayer composite hyperbolic metamaterial (HMM), graphene thin-film on the D-shaped fiber SPR sensor with the improved sensitivity up to 4 461 nm/RIU. However, the above methods change the external relative refractive index (RI) from the surface of the gold film to make the external effective RI closer to the base RI so as to improve the RI sensitivity of the device [32–35]. Complex surface modification methods can enhance the base sensitivity of the sensor, but the limited improvement often results in the extra complexity for the subsequent modification of the biochemical sensor. The RIs of fused silica (SiO<sub>2</sub>) [34] and polymethyl methacrylate (PMMA) [35] are too high to serve as substrates for highly sensitive SPR biosensors.

In order to overcome this hurdle, we proposed the use of low-index material substrates [36, 37]. A promising candidate was a polymer optical fiber (POF, GigaPOF-50SR) with a core that had a low RI of 1.359. Therefore, a new type of D-shaped fiber-optic SPR IgG sensor was proposed with the high sensitivity, simple fabrication, and potential low cost. In addition, the simple sensor structure was convenient for the modification of biomass in the later stage. The human IgG and goat anti-human IgG were used for the antigen and antibody experiments.

## 2. Materials and principle

A section of the side polished POF with the 50-nm-thick gold film was sealed in a microfluidic channel (Fig.1), where the yellow zone represents the coated gold film, as shown in Fig. 1. This area was functionalized with the goat anti-human IgG for human IgG detection.

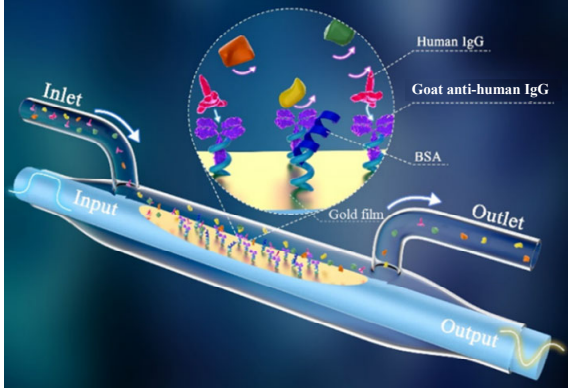


Fig. 1 Schematic view of the proposed sensor that was sealed in a microfluidic channel.

## 2.1 Materials

The 11-Mercaptoundecanoic acid (MUA), bovine serum albumin (BSA), N-(3-Dimethylaminopropyl)-N-ethyl carbodiimide hydrochloride (EDC), and N-Hydroxy succinimide (NHS) were purchased from Sigma-Aldrich. The goat anti-human IgG antibody and human IgG were purchased from Shenzhen Anyan Biotechnology Co., Ltd. Phosphate buffered saline (PBS, pH=7.4) was purchased from Coolaber Science & Technology. The piranha solution [1:3 (v/v) mixture of 30% H<sub>2</sub>O<sub>2</sub> and 98% H<sub>2</sub>SO<sub>4</sub>] and NaOH solution (10 mM) were prepared with ultra-pure water. All of the chemicals were of the analytical reagent grade. GigaPOF-50SR optical fibers with the 50 μm core and low core RI were purchased from Chromis Technologies Inc.

## 2.2 Principle

The SPR is the coupling effect between the plasma waves and evanescent field of the light wave on a metallic surface. The prism coupling model proposed by A. Otto [38] and E. Kretschmann *et al.* [39] allows the SPR theory to be applied here as follows. A total internal reflection of light occurs at the interface between a fiber core and a gold film surface. At the interface, the evanescent wave leaks to the gold film from the fiber core and generates a plasma wave. When the wave vector ( $k_{ev}$ ) of the

core mode in the axial direction is equal to the propagation constant ( $k_{sp}$ ) of the plasma mode, the phenomenon of the SPR occurs. It can be described by

$$k_{ev} = \frac{\omega_{ev}}{c} \sqrt{\epsilon_0 \sin^2 \theta}, \quad k_{sp} = \frac{\omega_{sp}}{c} \sqrt{\frac{\epsilon_m \epsilon_d}{\epsilon_m + \epsilon_d}} \quad (1)$$

where  $\omega_{sp}$  and  $\omega_{ev}$  are the plasma frequency and the frequency of the incident light, respectively.  $c$  represents the speed of light in vacuum,  $\theta$  is the incidence angle, and  $\epsilon_0$  and  $\epsilon_m$  are the dielectric constants of the optical fiber and gold, respectively.  $\epsilon_d$  is the dielectric constant of the external material, which is related to the external RI. Therefore, it can be deduced that the RI sensitivity can be expressed as

$$S = \frac{\lambda_{ev}^3 \omega_{sp}^2}{8\pi^2 - c^2 \epsilon_0 \sin^2 \theta} \quad (2)$$

where  $S$  is the RI sensitivity of the device,  $\lambda_{ev}$  is the resonant wavelength, and  $n_d$  is the RI of the external medium. For the same external medium and the same metal,  $n_d$ ,  $\omega_{sp}$ , and  $\epsilon_m$  are all constants, and the incident angle  $\theta$  is also a constant for the optical fiber. According to the dispersion curve, it can be found that the lower the RI of the substrate is, the greater redshift of the resonance wavelength is. Therefore, to significantly improve the sensitivity of similar structures, relatively low RI materials should be used. A specialty POF with the RI of its core based on the CYTOP® material is only 1.357, which is expected to be used for preparing highly sensitive SPR devices. Simulation of this POF is conducted to study the relationship between the RI sensitivity and absorptivity under varying gold film conditions. As shown in Fig. 2(a), when the thickness of the gold film increases, the sensitivity increases but the absorption rate decreases. This indicates that the resonance peak becomes shallower, which is unfavorable for accurately resolving the spectral shift. Therefore, it is better to choose a gold film of

50 nm in thickness. The simulated spectrum is shown in Fig. 2(b). The RI sensitivity of the proposed device can reach 30432 nm/RIU, while a silica fiber under the same conditions can only achieve 1133.70 nm/RIU. There is a 26-fold difference, which indicates a significant increase in the sensitivity by the use of the POF fiber.

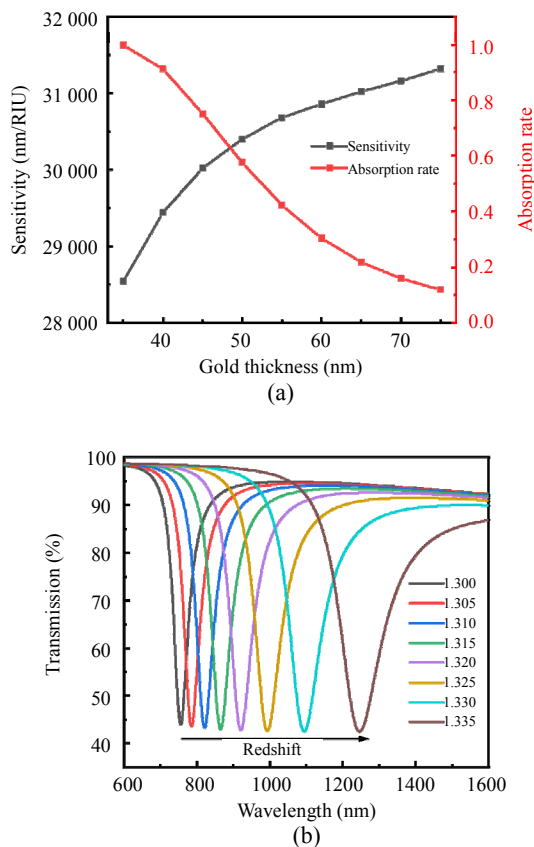


Fig. 2 Simulation of (a) variation in the sensitivity and absorbance for the gold film thickness increasing from 30 nm to 80 nm, and (b) RI spectra of a POF based SPR device with the 50-nm-thick gold film in different surrounding RIs.

### 3. Experiment

#### 3.1 Sensor fabrication

The D-shaped POF used in the experiment was fabricated by the wheel-polishing technique [34]. Firstly, a section of the POF was side-polished by the wheeled sandpaper, where the cladding and a portion of the fiber core were removed by side polishing to obtain an exposed-core sensing area with a length of 5 mm, and the D-shaped POF was

rinsed with deionized (DI) water to remove surface contaminants. The D-shaped POF was then coated with a 50-nm-thick gold film through magnetron sputtering. Subsequently, the D-shaped POF was washed with ethanol and DI water to remove surface impurities, dried with nitrogen at room temperature, and stored in a dust-free environment.

Finally, the bonding efficiency of the biosensor depends on the property of the D-shaped surface, the number of binding sites, and the type of biomolecules. To recognize the human IgG, the biosensor was modified by the goat anti-human IgG. Figure 3 shows the modification process for the proposed sensor. The gold surface of the POF was first coated with the MUA (1 mM, ethanol solution) at room temperature for 12 h, followed by rinsing with ethanol and dried by N<sub>2</sub> gas. The carboxylic group of the thiolate surface was activated with an aqueous solution of a mixture of the EDC/NHS (0.4 mM/0.1 mM) at room temperature for 30 min. Followed by being immersed into the goat anti-human IgG solution (100 µg/mL) for 1 h, to ensure the proper orientation and improve the combination between the goat anti-human IgG and human IgG. Finally, the sensor was soaked into the BSA solution (10 mg/mL) for 30 min to prevent the combination of carboxyl groups on the surface of the MUA-Au film and the human IgG. This completed the functionalization of the sensor surface as an immunosensor for the detection of the target human IgG.

#### 3.2 Experimental system and origin spectrum analysis

The experimental setup shown in Fig. 4 consists of a white light source (HL100, Idea Optics), spectrometers with a detection range from 900 nm to 1700 nm (NIRQuest512, Ocean Optics) and a detection range from 200 nm to 1100 nm (Ocean Optics), respectively, and a fluidic system comprising a peristaltic pump (LSP02-1B Longer Pump) and a self-designed flow-cell. A microfluidic channel of approximately 1 cm in length was

fabricated, and a microfluidic syringe pump was used to control the flow rate of liquid in the

microfluidic channel with the flow rate regulated at 5.0265  $\mu\text{L}/\text{mL}$ .

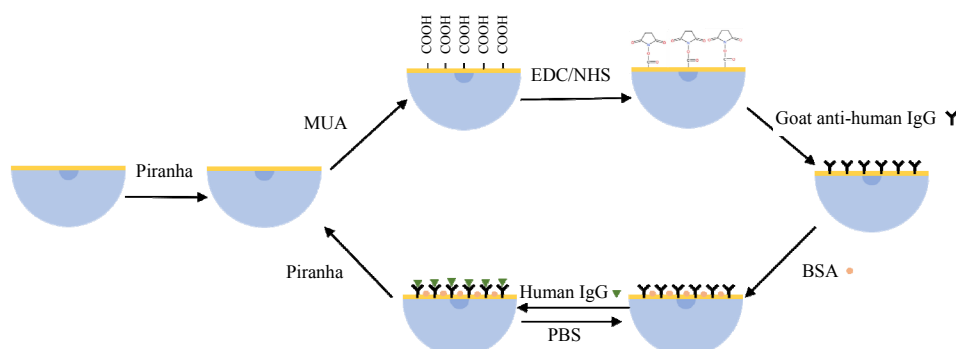


Fig. 3 Flowchart of functionalization and human IgG detection of the SPR biosensor.

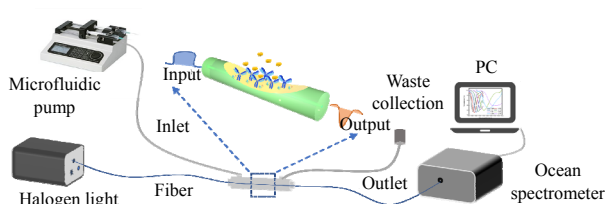


Fig. 4 Schematic diagram of the experiment setup.

During experiments, the light emitted by the white light source was coupled into the POF, in order to excite the SPR in the sensing area. The transmitted light acquired by the spectrometer was digitized and normalized with respect to the average intensity of the source, which revealed the resonance produced by the SPR. As the biochemical interactions on the gold surface induced a change in the external RI, they could be monitored through the corresponding shift of the nominal resonant wavelength.

## 4. Results and discussion

### 4.1 RI response

To evaluate the sensing performance of the D-shaped fiber SPR device, separate RI tests were conducted based on the single mode fiber (SMF) and POF, respectively. The thickness and polished length of the residual D-shaped zone were 68  $\mu\text{m}$  and 5 mm, and 245  $\mu\text{m}$  and 5 mm for SMF and POF fibers, respectively. And the thickness of the coated gold film was 50 nm for both cases. A set of

RI-matching solutions was used for the RI sensitivity measurement. As shown in Fig. 5(a), the SPR resonance peak of the SMF device was located at 550 nm–800 nm with an overall wavelength shift of 173.62 nm in the 1.30–1.39 RI range. As seen in Fig. 5(b), the resonance peak of the POF device was located at 800 nm–1400 nm with a peak wavelength shift of 571.15 nm in the 1.30–1.34 RI conditions. Therefore, the RI response of SPR devices based on SMF and POF fibers were compared in the RI range of 1.30–1.34. For an external RI of 1.335, the SPR resonance peak of the SMF device was located at 615.16 nm, and the RI sensitivity was 1133.70 nm/RIU based on the third-order polynomial fit, while the SPR resonance peak of the POF device was located at 1375.87 nm and the RI sensitivity was 30049.61 nm/RIU. The difference between the two resonance peaks was 760.81 nm, while the RI sensitivity of the POF device was 26.5 times higher than that of the SMF device. This phenomenon stemmed from the mechanism of the SPR that based on a conventional prism structure, where the closer the RI of the external environment was to the RI of the prism was, the higher the RI sensitivity was [36]. The SMF fiber is generally made from fused silica with an RI of 1.46, while the POF used here was made of Teflon with an RI of 1.35, and thus the sensitivity of the POF device was much higher than that of the SMF device in an aqueous solution-based environment.

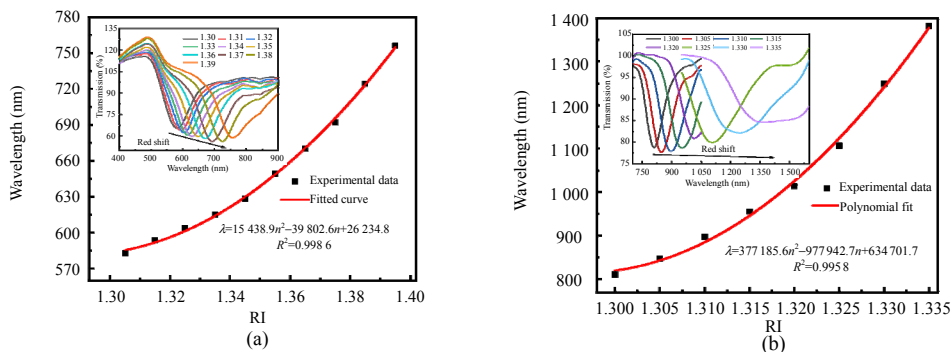


Fig. 5 RI response of the (a) SMF and (b) POF.

During the measurement process, there were many factors that affected the measurement result of the sensor, such as temperature fluctuations. The concentration of the solution would also cause a shift in the resonant wavelength. In the actual measurement environment, the temperature of the IgG was very close to the body temperature. To study the impact of temperature changes, the

sensor was used to perform temperature measurement in the range of 20 °C–39 °C. The results are shown in Fig. 6, and the temperature sensitivity of SMF and POF based SPR devices were found to be  $-0.13 \text{ nm}/^\circ\text{C}$  and  $-0.39 \text{ nm}/^\circ\text{C}$ , respectively. Therefore, the wavelength shift of the sensor due to temperature changes could be neglected.

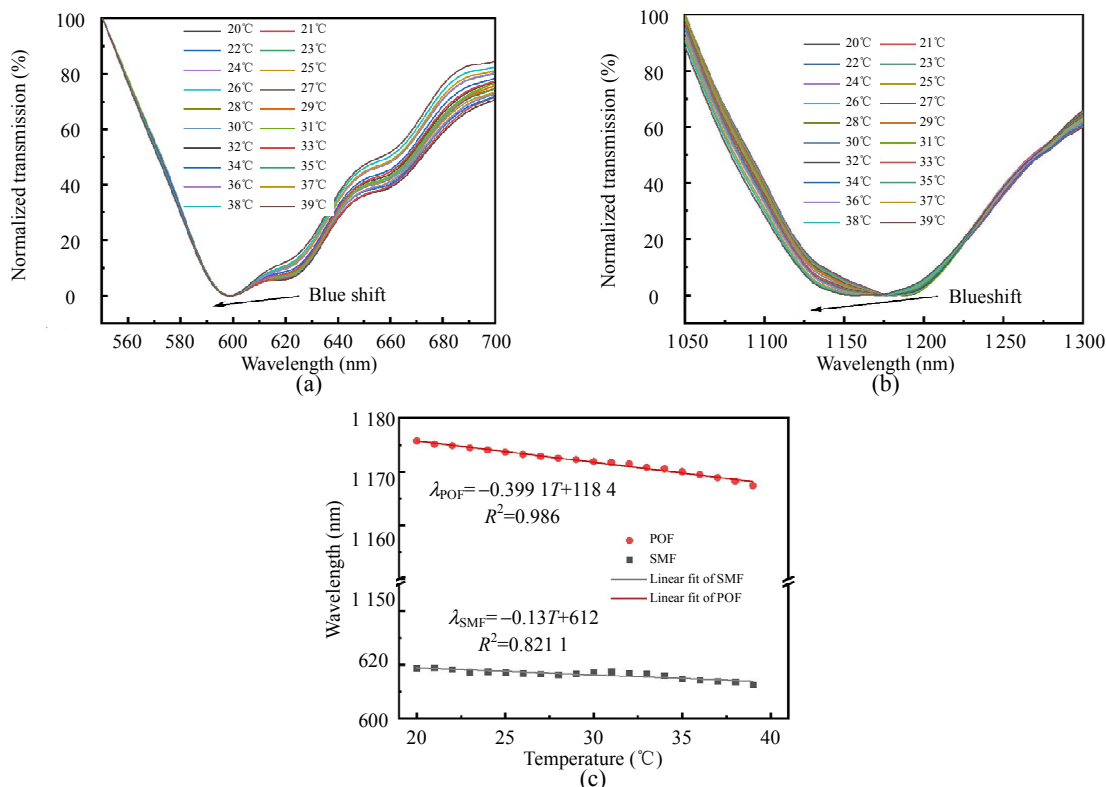


Fig. 6 Spectral evolution of the SPR device based on the (a) SMF and (b) POF with temperature increasing from 20 °C to 39 °C, (c) resonant wavelength shift versus temperature, where the linear fitting shows the temperature sensitivity.

## 4.2 Human IgG detection

Firstly, the surface of the POF fiber based SPR device was functionalized, and the human IgG was modified on the surface of the gold film according to the modification flowchart shown in Fig. 3 for the subsequent test of the human IgG with different concentrations. Figure 7 shows the resonant wavelength evolution and typical transmission spectra during the surface functionalization and the antigen-antibody reaction process. The initial resonant wavelength in the pure PBS was located at 1264.6 nm. In the process of surface functionalization, the resonant wavelength during the EDC/NHS process slowly shifted to longer

wavelengths, then the surface was modified with the goat anti-human IgG, and the resonant wavelength quickly shifted to 1290.4 nm. When the redundant sites were blocked with the BSA, the resonant wavelength stabilized at 1295.2 nm. The total wavelength shift exceeded 30.4 nm during the entire functionalization process. Then, using the 10  $\mu\text{g}/\text{mL}$  human IgG as an attempt, the resonant wavelength redshifted rapidly and finally settled at 1318.1 nm. The total wavelength shift was about 24.4 nm. As seen clearly in Fig. 7(b), the entire spectrum redshifted during the experiment, which indicated that this process indeed could be monitored by the D-shaped POF device in real time.

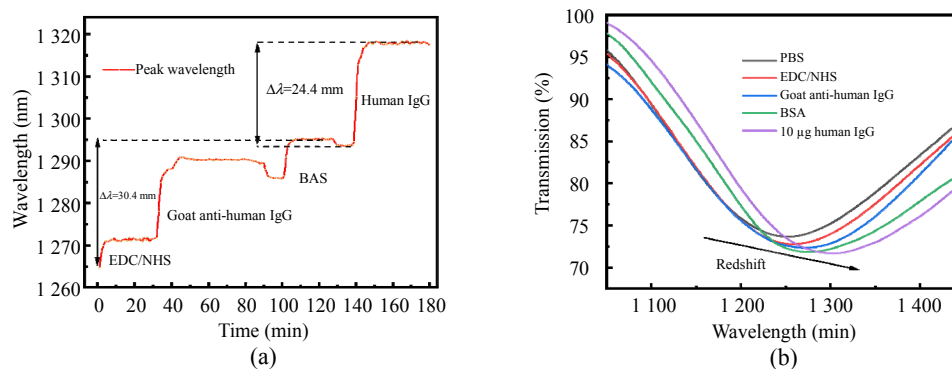


Fig. 7 Transient and spectral responses (a) resonant wavelength evolution and (b) typical transmission spectra during surface functionalization and antigen-antibody reaction.

Subsequently, human IgG solutions of different concentrations were slowly injected into the microfluidic channel, each for 30 min, and the transmission spectrum was recorded every 2 min, as shown in Fig. 8(a). In the first 6 min, the wavelength shifted abruptly, and then the wavelength remained essentially the same over time. After 10 min, there was the negligible change in resonant wavelengths, which meant that the human IgG and goat anti-human IgG were fully bound. The resonant wavelengths redshifted with increasing concentrations of the human IgG, which ranged from 0.5  $\mu\text{g}/\text{mL}$  to 80  $\mu\text{g}/\text{mL}$ . As is well known, it is difficult to completely clean out the human IgG that is bound on the surface of the Au film using the PBS.

Thus, the sensing area was rinsed using the PBS for over 20 min to achieve that most of the bound human IgG could be removed and the transmission spectrum could be restored. Moreover, the IgG solution was tested in the order of concentration increasing to reduce the accumulative effect of insufficient dissociation by using the PBS. During human IgG detection, the sensor could be regenerated using the PBS solution for more than 10 times. After human IgG detection, the sensor could also be regenerated by repeatedly dissociating biomolecular membranes from the piranha solution for more than 3 times. From the practical point of view, the device exhibited sufficient repeatability for human IgG detection in the case of the use at the

point of care. The resonance wavelength shifted as a function of the human IgG concentration is fitted in Fig. 8(b), with average error bars of 1.35 nm that could be mainly attributed to the fluctuation of the white light source. The highest sensitivity could be represented by the optical response between concentrations of 30  $\mu\text{g/mL}$  and 40  $\mu\text{g/mL}$ , which was 2.01 nm/( $\mu\text{g/mL}$ ).

$$\text{LoD} = \frac{3\sigma}{S} \tag{3}$$

where  $\sigma$  represents the standard deviation and  $S$  is the sensitivity. According to (3), the limit of detection (LoD) of the sensor could be estimated to be below 245.4 ng/mL. Table 1 lists the comparison of the proposed sensor with other IgG sensors previously reported.

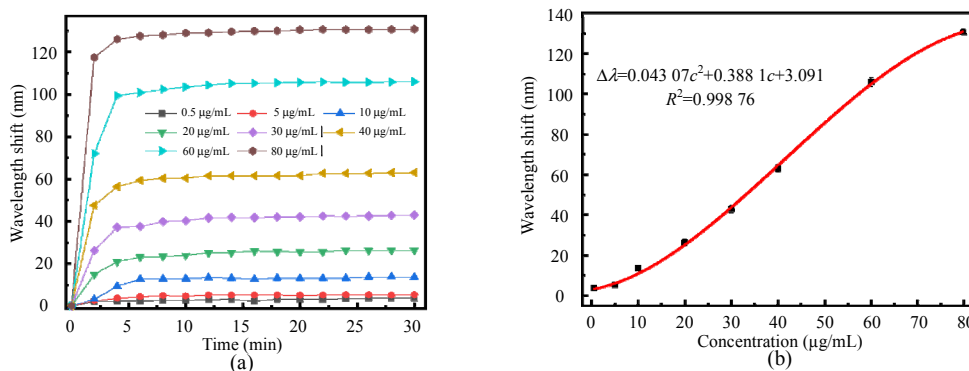


Fig. 8 Concentration measurement: (a) SPR wavelength shift as a function of time during human IgG detection and (b) total wavelength shift with curve fitting for concentrations ranging from 0.5  $\mu\text{g/mL}$  to 80  $\mu\text{g/mL}$ .

Table 1 Comparison of the proposed sensor with other previously reported IgG sensors.

Sensing method	Range ( $\mu\text{g/mL}$ )	LoD ( $\mu\text{g/mL}$ )	Ref.
GO/Ag-coated polymer cladding	5–30	0.498 5	[40]
Polydopamine-modified SPR	5–100	0.9	[41]
Multimode fiber-no-core fiber-multimode fiber structure SPR	2–250	1.75	[42]
Elliptical core helical intermediate-period fiber grating	10–100	4.7	[43]
H-shaped optical fiber SPR	10–100	3.4	[44]
$\Omega$ -shaped fiber optic LSPR	$4.5 \times 10^5$ – $2.2 \times 10^9$ copies/mL	9.2 pM	[45]
J-shaped optical fiber localized surface plasmon resonance	$1.0 \times 10^2$ – $1.0 \times 10^8$ CFU/mL	45.23 CFU/mL	[46]
Low index polymer optical fiber SPR	0.5–80.0	0.245 4	This work

### 4.3 Stability and specificity of the sensor

Figure 9 shows the stability of the sensor. The amount of the wavelength shift was relatively stable, and the maximum spectral wavelengths fluctuation was 0.855 nm. Noise accounted for 0.07% of the total wavelength shift. The standard deviation of the shift was 0.1644 nm, indicating that the sensor had the reasonably good stability. In order to confirm the selectivity of the sensor, the analytes of the human IgG and rabbit IgG with the same concentration were also tested for comparison, and the resonant wavelength shift was recorded under the same conditions, as shown in Fig. 10. It was clear that the human IgG induced a significantly larger wavelength shift than other substances within the same concentration range. These results confirmed that the proposed sensor showed the good selectivity for human IgG detection.

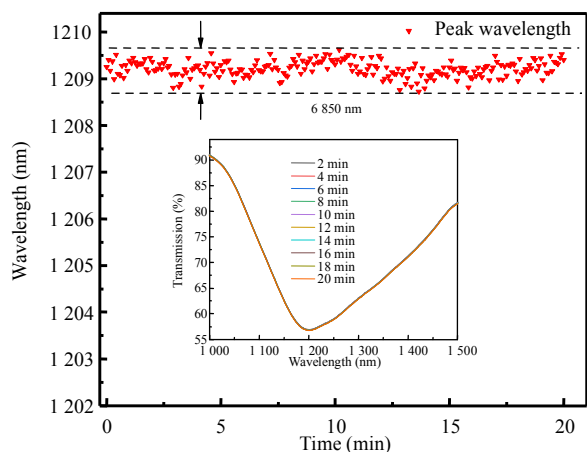


Fig. 9 Spectral stability of the sensor measured over 20 min.

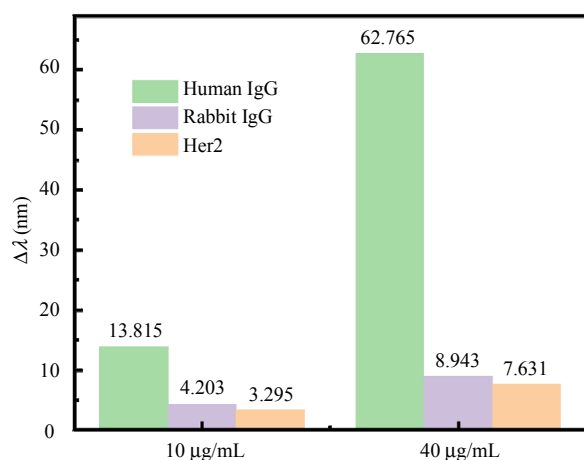


Fig. 10 Specific binding test. Note that the vertical axis denotes the wavelength shift relative to the initial wavelength in the pure PBS solution.

## 5. Conclusions

We fabricated a D-shaped fiber-optic SPR biosensor, which consisted of a uniform 50-nm-thick gold film coated on a low-index POF. The sensor demonstrated the high sensitivity compared to the state-of-the-art, with a sensitivity of 30 049.61 nm/RIU which was 26.5 times higher than that of the SMF device. In addition, piranha solution immersion and cleaning enabled the reuse of the POF based SPR device for over 3 times. The method showed the good antibody immobilization efficiency, high sensitivity, and low LoD value of 245.4 ng/mL for human IgG detection. In consideration of the simple fabrication process, high performance, and robustness, the D-shaped POF

fiber based SPR biosensor has the great potential for quantifying the human serum and plasma.

## Acknowledgment

This work was supported by the National Natural Science Foundation of China (Grant No. 62275172); Natural Science Foundation of Guangdong Province (Grant No. 2023A1515012893); Science, Technology, and Innovation Commission of Shenzhen Municipality (Grant Nos. KQTD20221101093605019 and JCYJ20220818095615034); Shenzhen Key Laboratory of Ultrafast Laser Micro/Nano Manufacturing (Grant No. ZDSYS20220606100405013); Research Start-Up Fund for High-End Talent at Shenzhen University.

## Declarations

**Conflict of Interest** Yiping WANG is an editorial board member for Photonic Sensors and was not involved in the editorial review, or the decision to publish this article. All authors declare that there are no competing interests.

**Permissions** All the included figures, tables, or text passages that have already been published elsewhere have obtained the permission from the copyright owner(s) for both the print and online format.

**Open Access** This article is distributed under the terms of the Creative Commons Attribution 4.0 International License (<http://creativecommons.org/licenses/by/4.0/>), which permits unrestricted use, distribution, and reproduction in any medium, provided you give appropriate credit to the original author(s) and the source, provide a link to the Creative Commons license, and indicate if changes were made.

## References

- [1] L. A. Cavacini, M. Kennel, E. V. Lally, M. R. Posner, and A. Quinn, "Human immunoglobulin production in immunodeficient mice: enhancement by immunosuppression of host and in vitro activation of human mononuclear cells," *Clinical & Experimental Immunology*, 1992, 90(1): 135–140.
- [2] U. Artus, E. W. Herbst, J. A. Rump, and H. H. Peter, "Defects in the immunoglobulin producing cells in bone marrow of patients with variable immunodeficiency syndrome," *Immunitat und Infektion*, 1995, 23(2): 69–71.

- [3] S. Barmettler, M. S. Ong, J. R. Farmer, H. Choi, and J. Walter, "Association of immunoglobulin levels, infectious risk, and mortality with rituximab and hypogammaglobulinemia," *JAMA Network Open*, 2018, 1(7): e184169.
- [4] A. Epp, K. C. Sullivan, A. B. Herr, and R. T. Strait, "Immunoglobulin glycosylation effects in allergy and immunity," *Current Allergy and Asthma Reports*, 2016, 16: 79.
- [5] P. G. E. Kennedy, M. Graner, T. Pointon, X. Li, K. Tanimoto, K. Dennison, *et al.*, "Aberrant immunoglobulin G glycosylation in multiple sclerosis," *Journal of Neuroimmune Pharmacology*, 2022, 17(1–2): 218–227.
- [6] K. Brockow, "Detection of drug-specific immunoglobulin E (IgE) and acute mediator release for the diagnosis of immediate drug hypersensitivity reactions," *Journal of Immunological Methods*, 2021, 496: 113101.
- [7] Y. T. Tseng, Y. J. Chuang, Y. C. Wu, C. S. Yang, M. C. Wang, and F. G. Tseng, "A gold-nanoparticle-enhanced immune sensor based on fiber optic interferometry," *Nanotechnology*, 2008, 19(34): 345501.
- [8] L. H. Chen, C. C. Chan, K. Ni, P. B. Hu, T. Li, W. C. Wong, *et al.*, "Label-free fiber-optic interferometric immunosensors based on waist-enlarged fusion taper," *Sensors and Actuators B: Chemical*, 2013, 178: 176–184.
- [9] F. Chiavaioli, P. Biswas, C. Trono, S. Bandyopadhyay, A. Giannetti, S. Tombelli, *et al.*, "Towards sensitive label-free immunosensing by means of turn-around point long period fiber gratings," *Biosensors and Bioelectronics*, 2014, 60: 305–310.
- [10] Y. Chen and H. Ming, "Review of surface plasmon resonance and localized surface plasmon resonance sensor," *Photonic Sensors*, 2012, 2(1): 37–49.
- [11] B. T. Wang and Q. Wang, "An interferometric optical fiber biosensor with high sensitivity for IgG/anti-IgG immunosensing," *Optics Communications*, 2018, 426: 388–394.
- [12] S. Q. Hu, Y. F. Chen, Y. Chen, L. Chen, H. D. Zheng, N. H. Azeman, *et al.*, "High-performance fiber plasmonic sensor by engineering the dispersion of hyperbolic metamaterials composed of Ag/TiO<sub>2</sub>," *Optics Express*, 2020, 28(17): 25562–25573.
- [13] H. Bhardwaj, G. Sumana, and C. A. Marquette, "A label-free ultrasensitive microfluidic surface plasmon resonance biosensor for aflatoxin B-1 detection using nanoparticles integrated gold chip," *Food Chemistry*, 2020, 307: 125530.
- [14] S. Balbinot, A. M. Srivastav, J. Vidic, I. Abdulhalim, and M. Manzano, "Plasmonic biosensors for food control," *Trends in Food Science & Technology*, 2021, 111: 128–140.
- [15] R. Gu, Y. Duan, Y. Li, and Z. Luo, "Fiber-optic-based biosensor as an innovative technology for point-of-care testing detection of foodborne pathogenic bacteria to defend food and agricultural product safety," *Journal of Agricultural and Food Chemistry*, 2023, 71(29):10982–10988.
- [16] C. R. Lawrence, N. J. Geddes, D. N. Furlong, and J. R. Sambles, "Surface plasmon resonance studies of immunoreactions utilizing disposable diffraction gratings," *Biosensors and Bioelectronics*, 1996, 11(4): 389–400.
- [17] F. Chiavaioli, P. Zubiato, I. Del Villar, C. R. Zamarreno, A. Giannetti, S. Tombelli, *et al.*, "Femtomolar detection by nanocoated fiber label-free biosensors," *ACS Sensors*, 2018, 3(5) 936–943.
- [18] E. N. Primo, M. J. Kogan, H. E. Verdejo, S. Bollo, M. D. Rubianes, and G. A. Rivas, "Label-free graphene oxide-based surface plasmon resonance immunosensor for the quantification of galectin-3, a novel cardiac biomarker," *ACS Applied Materials & Interfaces*, 2018, 10(28): 23501–23508.
- [19] Y. Qian, Y. Zhao, Q. L. Wu, and Y. Yang, "Review of salinity measurement technology based on optical fiber sensor," *Sensors and Actuators B: Chemical*, 2018, 260: 86–105.
- [20] Y. Zhao, R. J. Tong, F. Xia, and Y. Peng, "Current status of optical fiber biosensor based on surface plasmon resonance," *Biosensors and Bioelectronics*, 2019, 142: 111505.
- [21] W. Luo, J. Meng, X. Li, Q. Xie, D. Yi, Y. Wang, *et al.*, "Temperature effects on surface plasmon resonance sensor based on side-polished D-shaped photonic crystal fiber," *Measurement*, 2021, 181: 109504.
- [22] C. Li, Z. Li, S. L. Li, Y. N. Zhang, B. P. Sun, Y. H. Yu, *et al.*, "LSPR optical fiber biosensor based on a 3D composite structure of gold nanoparticles and multilayer graphene films," *Optics Express*, 2020, 28(5): 6071–6083.
- [23] B. Sun and Y. P. Wang, "High-sensitivity detection of IgG operating near the dispersion turning point in tapered two-mode fibers," *Micromachines*, 2020, 11(3): 270.
- [24] P. Wang, L. Bo, and Y. Semenova, "Optical microfiber based photonic components and their applications in label-free biosensing," *Biosensors*, 2015, 5(3) 471–499.
- [25] Y. N. Zhang, S. Y. E, B. R. Tao, Q. L. Wu, and B. Han, "Reflective SPR sensor for simultaneous measurement of nitrate concentration and temperature," *IEEE Transactions on Instrumentation and Measurement*, 2019, 68(11): 4566–4574.
- [26] J. X. Sun, S. Z. Jiang, J. H. Xu, Z. Li, C. H. Li, Y. Jing, *et al.*, "Sensitive and selective surface plasmon resonance sensor employing a gold-supported graphene composite film/D-shaped fiber for dopamine detection," *Journal of Physics D-Applied Physics*, 2019, 52(19): 195402.

- [27] N. Cennamo, F. Arcadio, A. Minardo, D. Montemurro, and L. G. Zeni, "Experimental characterization of plasmonic sensors based on lab-built tapered plastic optical fibers," *Applied Sciences*, 2020, 10(12): 4389.
- [28] F. Wang, Y. Zhang, M. Lu, Y. Du, M. Chen, S. Meng, *et al.*, "Near-infrared band gold nanoparticles-Au film 'hot spot' model based label-free ultratrace lead (II) ions detection via fiber SPR DNAzyme biosensor," *Sensors and Actuators B: Chemical*, 2021, 337: 129816.
- [29] X. Xiong, Y. F. Chen, H. Wang, S. Q. Hu, Y. H. Luo, J. L. Dong, *et al.*, "Plasmonic interface modified with graphene oxide sheets overlayer for sensitivity enhancement," *ACS Applied Materials & Interfaces*, 2018, 10(41): 34916–34923.
- [30] A. K. Sharma, B. Kaur, and V. A. Popescu, "On the role of different 2D materials/heterostructures in fiber-optic SPR humidity sensor in visible spectral region," *Optical Materials*, 2020, 102: 109824.
- [31] C. Li, J. Gao, M. Shafi, R. Liu, Z. Zha, D. Feng, *et al.*, "Optical fiber SPR biosensor complying with a 3D composite hyperbolic metamaterial and a graphene film," *Photonics Research*, 2021, 9(3): 379–388.
- [32] J. Wang, G. Y. Chen, X. Wu, H. Xu, T. M. Monro, T. Liu, *et al.*, "Light-sheet skew ray-enhanced localized surface plasmon resonance-based chemical sensing," *ACS Sensors*, 2020, 5(1): 127–132.
- [33] M. Cardoso, A. Silva, A. Romeiro, M. Giraldo, J. Costa, J. Santos, *et al.*, "Second-order dispersion sensor based on multi-plasmonic surface resonances in D-shaped photonic crystal fibers," *Photonics*, 2021, 8(6): 181.
- [34] J. Zhao, S. Cao, C. Liao, Y. Wang, G. Wang, X. Xu, *et al.*, "Surface plasmon resonance refractive sensor based on silver-coated side-polished fiber," *Sensors and Actuators B: Chemical*, 2016, 230: 206–211.
- [35] W. Gong, S. Z. Jiang, Z. Li, C. H. Li, J. H. Xu, J. Pan, *et al.*, "Experimental and theoretical investigation for surface plasmon resonance biosensor based on graphene/Au film/D-POF," *Optics Express*, 2019, 27(3) 3483–3495.
- [36] S. Q. Cao, Y. Shao, Y. Wang, T. S. Wu, L. F. Zhang, Y. J. Huang, *et al.*, "Highly sensitive surface plasmon resonance biosensor based on a low-index polymer optical fiber," *Optics Express*, 2018, 26(4) 3988–3994.
- [37] T. Wu, Y. Shao, Y. Wang, S. Q. Cao, W. P. Cao, F. Zhang, *et al.*, "Surface plasmon resonance biosensor based on gold-coated side-polished hexagonal structure photonic crystal fiber," *Optics Express*, 2017, 25(17): 20313–20322.
- [38] A. Otto, "Excitation of nonradiative surface plasma waves in silver by the method of frustrated total reflection," *Zeitschrift für Physik A Hadrons and Nuclei*, 1968, 216(4): 398–410.
- [39] E. Kretschmann and H. Raether, "Notizen: radiative decay of non radiative surface plasmons excited by light," *Zeitschrift für Naturforschung A*, 1968, 23(12): 2135–2136.
- [40] A. A. Rifat, G. A. Mahdiraji, D. M. Chow, Y. G. Shee, R. Ahmed, and F. R. M. Adikan, "Photonic crystal fiber-based surface plasmon resonance sensor with selective analyte channels and graphene-silver deposited core," *Sensors*, 2015, 15(5): 11499–11510.
- [41] S. Shi, L. Wang, R. Su, B. Liu, R. Huang, W. Qi, *et al.*, "A polydopamine-modified optical fiber SPR biosensor using electroless-plated gold films for immunoassays," *Biosensors and Bioelectronics*, 2015, 74: 454–460.
- [42] Y. Zheng, T. Lang, B. Cao, J. Jin, R. Dong, and H. Feng, "Fiber optic SPR sensor for human Immunoglobulin G measurement based on the MMF-NCF-MMF structure," *Optical Fiber Technology*, 2018, 46: 179–185.
- [43] J. Zhong, S. Liu, T. Zou, W. Yan, M. Zhou, B. Liu, *et al.*, "All fiber-optic immunosensors based on elliptical core helical intermediate-period fiber grating with low-sensitivity to environmental disturbances," *Biosensors*, 2022, 12(2): 99.
- [44] Y. Huang, Y. Wang, G. Xu, X. Rao, J. Zhang, X. Wu, *et al.*, "Compact surface plasmon resonance IgG sensor based on H-shaped optical fiber," *Biosensors*, 2022, 12(3): 141.
- [45] Z. Luo, Y. Cheng, L. He, Y. Feng, Y. Tian, Z. Chen, *et al.*, "T-shaped aptamer-based LSPR biosensor using  $\Omega$ -shaped fiber optic for rapid detection of SARS-CoV-2," *Analytical Chemistry*, 2023, 95(2): 1599–1607.
- [46] W. Ning, S. Hu, and C. Zhou, "An ultrasensitive J-shaped optical fiber LSPR aptasensor for the detection of *Helicobacter pylori*," *Analytica Chimica Acta*, 2023, 1278: 341733.